



ARTICLE

Effects of Hydrothermal Environment on the Deformation of the Thin Bamboo Bundle Veneer Laminated Composites

Ge Wang, Linbi Chen, Haiying Zhou*, Shanyu Han and Fuming Chen*

Department of Bio-Materials, Key Laboratory of Bamboo and Rattan Science and Technology of the State Forestry Administration, International Centre for Bamboo and Rattan, Beijing, 100102, China

*Corresponding Authors: Fuming Chen. Email: fuming@icbr.ac.cn; Haiying Zhou. Email: 15288423522@163.com

Received: 23 June 2022 Accepted: 26 July 2022

ABSTRACT

To overcome warping in thin bamboo bundle veneer laminated composites (TBLC), their hydrothermal deformation characteristics were systematically investigated in this study. It was found that TBLCs accelerated the release of internal stress in the thickness direction in a hydrothermal environment, which increased their warpage. TBLCs showed increased warpage in the width and diagonal directions upon increasing the temperature. The warpage of Type E increased by 155.88% and 66.67% in the width and diagonal directions, respectively, when the temperature increased from 25°C to 100°C. The symmetrical TBLC with cross-lay-up and odd layers displayed better hydrothermal stability. We revealed that the deformation of the TBLCs could be regulated under the synergistic effect of water and temperature. These results provide a scientific basis for improving the uniformity of bamboo bundle composite materials and for developing thin bamboo bundle fiber composite materials with designable structures and controllable performance.

KEYWORDS

Thin bamboo bundle veneer laminated composites; deformation; hydrothermal environment; lay-up structure

1 Introduction

In recent years, innovative bamboo products have been continuously updated. On the basis of reconstituted bamboo, researchers have developed bamboo bundle veneer laminated composites (BLVL) with uniform density and stable quality [1–4]. However, BLVL has shortcomings such as excessive weight, excessive mechanical strength, low assembly efficiency, and poor connection performance. It is difficult to be used as a large-format material in the fields of wall panels, decoration and building structures. The thinning of conventional reconstituted bamboo products and the development of new thin, lightweight and non-deformable bamboo bundle composite materials to meet the market's demand for thin plates will have huge market prospects and unique advantages. As a plant fiber composite material, thin laminated bamboo bundle veneer composites (TBLC) are exposed to the natural environment during their use. They contain many tiny pores and hydrophilic functional groups (such as hydroxyls), which cause them to absorb water from humid environments. The motion of water molecules is closely related to temperature, and a higher temperature increases the motion of water molecules, especially under the coupled effects of temperature and moisture. This is due to differences in the sensitivity between pores,



fibers, and the resin matrix [5]. They easily generate internal stress, microcracks, and even large cracks through the bonding interface in thin laminated bamboo bundle veneer composites. This results in poor dimensional stability, warping, and a reduction in mechanical properties [6]. Deformation is one of the main factors affecting the service life of thin panels [7–9]. It is also a serious threat to product quality during secondary processing in the bamboo and wood industries. Therefore, it is very important to study the water absorption characteristics and deformation behavior of TBLCs in a hydrothermal environment and to predict the deformation of the composites in a hydrothermal environment.

Bamboo/wood fiber is a viscoelastic porous material. During composite fabrication, bamboo bundle veneers and wood veneers are subjected to pressure and temperature, causing internal stress. The compressed composites release internal stress under a hydrothermal environment due to moisture absorption, which causes thickness expansion. Shi et al. [10,11] considered that the hygroscopic thickness swelling was related to the initial thickness of panels and established a prediction model for the hygroscopic thickness of wood fiberboard and wood fiber/polymer composites under different temperatures and humidity conditions. They found that temperature had a great influence on the hygroscopic thickness swelling, while the prediction model showed low accuracy at high temperatures. Some scholars used the hygroscopic thickness prediction model developed by Shi and Gardner to study the hygroscopic thickness swelling process of different wood-plastic composites (WPCs). The results showed that the swelling model accurately predicted the hygroscopic swelling process of wood-plastic composites [12,13]. Many researchers have investigated the warping of asymmetric structural composite materials and laminated bamboo/wood lumber. It is believed that reasonable structural design can reduce the occurrence of panel deformation [14–18]. The water content gradient in the thickness direction generated by the symmetrical panel will also develop internal stresses and cause deformation [19–21]. Guan et al. [22] studied the hydrothermal effect of bamboo, wood, and bamboo-wood composite panels and obtained the hygroscopic swelling coefficient of bamboo and wood under different environments. Software was used to simulate the deformation of the panels under isothermal humidity. It was found that water had a very significant influence on panel deformation, but temperature had almost a negligible effect compared with water. More and more scholars used mathematical models to predict the warping deformation of bamboo and wood panels in a humid and hot environment [23]. Future development trends should carry out in-depth research on the warping of bamboo/wood composites in hydrothermal environments and use numerical methods to simulate and predict their deformation.

At present, the research on the hydrothermal properties of natural fiber composites has mainly focused on regulating the attenuation of mechanical properties. Research on the deformation has mostly focused on the deformation of asymmetric composites. In practical production and applications, bamboo and wood composites are generally prepared by symmetrical paving to prevent warping. Therefore, it is of great significance to study the deformation behavior of TBLCs with symmetrical structures in hydrothermal environments. This study mainly investigates the deformation behavior of TBLCs with different symmetrical laminated structures in different hydrothermal environments to explore their linear deformation and warping regulation under hydrothermal aging. It provides a theoretical basis for the long-term safe use of TBLCs in hydrothermal environments.

2 Materials and Methods

2.1 Materials

Bamboo (*Phyllostachys edulis*; 3~4 years old) was harvested from Yong'an, Fujian, China. Bamboo bundles were prepared by mechanical brooming of the bamboo shoots followed by air-drying until a moisture content (MC) of 10%~15% was achieved. The resulting bamboo bundles had a thickness of 2.0 mm. Poplar veneer (*Populus ussuriensis* Kom.) with a 10%~15% MC and a thickness of 1.0 mm was purchased from Cangzhou County, Hebei, China. A water-soluble phenol-formaldehyde (PF) resin with a

solids content of 45.40% was purchased from Beijing Taier Chemical Co., Ltd., China and used as an adhesive. The cotton thread with better performance is used as the connecting thread to weave the dried narrow and long bamboo bundle unit to prepare a whole bamboo bundle veneer, and the bamboo bundle veneer is used as the basic unit for manufacturing TBLC [2,24].

2.2 Preparation of TBLC

A CARVER M-3895 hot press (Carver, Inc., Wabash, IN, USA) was used to press the TBLC at 155°C for 30 min with 1 min of press closing, 14 min of pressure at the target thickness, and 15 min of press opening. TBLCs were prepared by laminating whole-sheet bamboo bundle veneers and wood veneers with different lay-up structures (Fig. 1). The dimensions and target density of the boards were 300 mm (length) × 150 mm (width) × 14 mm (thickness) and 1.0 g/cm³, respectively [24,25].

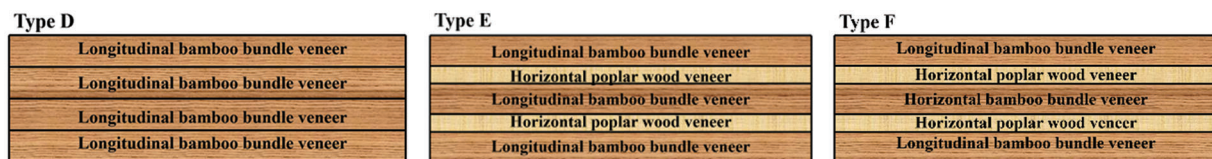


Figure 1: Different lay-up structures of TBLC

2.3 Methods

2.3.1 The Moisture Deformation and Water Absorption Test under Different Hydrothermal Conditions

Three different types of TBLC were cut to dimensions of 420 mm (L) × 240 mm (W) with 4 replicates and then placed in water baths at 25°C, 63°C, and 99°C, respectively. Then the mass, thickness, and warpage of the sample were measured over time. The thickness swelling was tested according to GB/T 17657-2013 “Test methods of evaluating properties of wood-based panels and surface decorated wood-based panels.” The side warpage and diagonal warpage were measured according to GB/T 18103-2013 “Engineered wood flooring” and GB/T 15036-2018 “Solid wood flooring.” The test was carried out in short measured intervals and with a high measurement frequency in the first 40 h. Then, a long measurement interval was performed until the quality and thickness of the sample stabilized.

2.3.2 Hygroscopic Swelling Coefficient Calculation

The hygroscopic swelling coefficient is a dimensionless constant in composite mechanics. When a composite absorbs water in a water-containing environment, the water absorption is represented by the available water absorption concentration, C . Orthotropic one-way panels undergo expansion deformation after absorbing moisture. The linear strain is generated in the main direction of the material, ε_T^H and ε_L^H , and the shear strain $\varepsilon_{LT}^H = 0$. According to the water absorption concentration (C), the hygroscopic swelling coefficient is defined as follows [23–26]:

$$\left. \begin{aligned} \beta_L &= \varepsilon_L^H / C \\ \beta_T &= \varepsilon_T^H / C \\ \beta_{LT} &= 0 \end{aligned} \right\} \quad (1)$$

where β_L and β_T are the longitudinal and transverse hygroscopic swelling coefficients, respectively; β_{LT} is the longitudinal and transverse hygroscopic angular coefficients. In wood science, the hygroscopic (water) expansion of bamboo or wood is expressed as the thickness swelling, i.e., the thickness difference between the absolute dried size and the size after absorption in air to the fiber saturation point (or the thickness difference between the absolute dried size and the size after the sample is immersed in water until reaching a stable size). The thickness swelling of bamboo and wood increases upon increasing the water absorption, but the swelling value is different under different moisture contents. Therefore, the thickness swelling of bamboo and wood is often regarded as having a linear relationship with the

moisture content [27]. The hygroscopic swelling coefficient of bamboo and wood is calculated as follows:

$$K_v(K_R, K_T) = \frac{E_v(E_R, E_T)}{W_{f.s.P}} \quad (2)$$

where K_V , K_R , and K_T are the volumetric, radial, and chordwise hygroscopic swelling coefficients (%), respectively; E_V , E_R , and E_T are the volume, radial, and chordwise thickness swelling (%), respectively; $W_{f.sp}$ is the moisture content at the fiber saturation point (%).

It can be seen from Eqs. (1) and (2) that the definition of the difference in the hygroscopic swelling coefficient between composite materials and wood science is an inconsistent expression of the material moisture content. In composite materials, the moisture content is expressed by the water absorption concentration. A composite is composed of fibers and a matrix. It is assumed that the mass of the dried material is M , the mass of the fiber is M_f , and the mass of the matrix is M_m , and $M = M_f + M_m$, the composite material after moisture absorption (water) increases ΔM , fibers increase ΔM_f , matrix increases ΔM_m , the water absorption concentration is calculated as follows:

$$C = \frac{\Delta M}{M} = \frac{\Delta M_f + \Delta M_m}{M_f + M_m} \quad (3)$$

The moisture content of a material is expressed by absolute moisture content (MC), which is calculated as follows:

$$MC = \frac{\Delta W}{W} = \frac{W - W_0}{W} \quad (4)$$

where W is the mass of wet wood, g, and W_0 is the mass of absolute dried wood, g.

According to the definition of the moisture content, the dried state in the composite material refers to the absolute dry state $W_0 = M$ (Eq. (4)). The moisture content of the material at each test point and strain in all directions under the constant-temperature state were measured and calculated. According to Eq. (2), within a certain moisture content range, the slope obtained by the linear fit of the moisture content (MC) and strain (ϵ) curve is the hygroscopic swelling coefficient (β) of the material.

2.3.3 Model Prediction for Thickness Swelling

Bamboo/wood fiber composites are sensitive to moisture and temperature changes. The thickness swelling model proposed by Shi et al. [10] can be used to quantitatively characterize and predict the thickness swelling of panels with different compositions and the sensitivity of the panels to temperature. The model is as follows:

$$TH(t) = \left(\frac{H_\infty}{H_0 + (H_\infty - H_0)e^{-K_{SR}t}} - 1 \right) \times 100 \% \quad (5)$$

where $TH(t)$ corresponds to the thickness swelling at time t , %, K_{SR} refers to the thickness swelling coefficient that characterizes the water-absorbing expansion rate, H_0 refers to the initial thickness, mm, and H_∞ is the final thickness, mm.

3 Results and Discussion

3.1 Thickness Swelling of TBLC in Different Hydrothermal Environments

Fig. 2 shows the thickness swelling (TS) curves of TBLCs with different laminate structures at 25°C, 63°C, and 100°C in a hydrothermal environment. The thickness swelling of the three composites all increased upon prolonging the time, and their increasing rates presented a parabolic shape that gradually stabilized. Upon increasing the temperature, less time was required to reach thickness swelling

equilibrium. The equilibrium thickness swelling and equilibrium thickness increased upon increasing the temperature. The thickness swelling of Type D was slightly higher than that of Type E with wood veneer in the early stage of water absorption. Upon prolonging the time, the thickness swelling of all composites gradually reached a stable state. Type D presented the least thickness swelling. Type F and Type E showed similar thickness swelling characteristics, and Type E was slightly smaller. Both presented a nearly linear relationship between the equilibrium TS and temperature under different hydrothermal conditions and less variability in data. This illustrates that the thickness swelling was less related to the lay-up structure of the TBLC and was mainly related to their composition, the reason is that the water absorption thickness expansion rate of poplar is higher than that of bamboo [28]. The Type D with a pure bamboo bundle veneer displayed a consistent and uniform swelling rate and quickly stabilized during water absorption. A higher temperature resulted in faster water absorption, so a steady state was reached faster. However, Type E and Type F contained wood veneer, which displayed greater thickness swelling than bamboo veneer; thus, Type E and Type F showed greater thickness swelling than Type D.

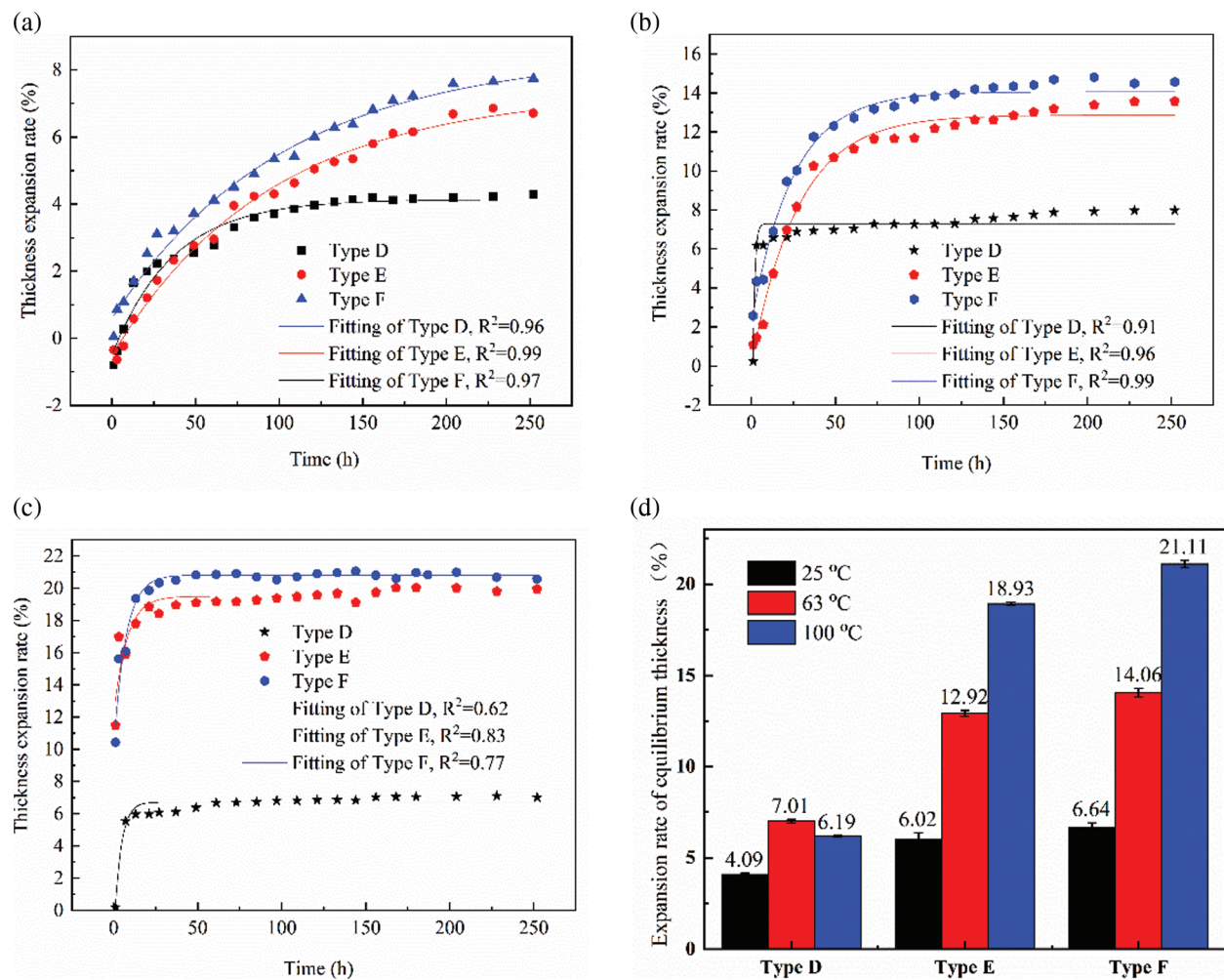


Figure 2: Thickness swelling of three types of TBLCs in 25°C (a), 63°C (b) and 100°C (c) hydrothermal environments. (d) The equilibrium thickness swelling of TBLC under different temperature

The thickness swelling model (Eq. (5)) was used to fit the thickness swelling data of the three composites under different hydrothermal conditions, and the fitting curves are shown in Fig. 2. The fitting curve of the thickness swelling provided a better fit at low temperatures with $R^2 \geq 95\%$ at 25°C and 63°C . All composites had $R^2 < 90\%$ at 100°C . This indicates that the model was suitable for predicting the thickness swelling of bamboo bundle fiber composite boards at low temperatures. A high temperature led to large deviations, thus requiring further corrections.

The thickness swelling coefficient (K_{SR}) of the TBLC can be calculated through the thickness swelling model, and the transverse hygroscopic swelling coefficient (β_{T}) of the TBLC can be obtained by the moisture content-strain fitting curve, as shown in Table 1. The thickness swelling coefficient obtained by the thickness swelling model and the hygroscopic expansion coefficient in the thickness direction obtained by the moisture content-strain fitting curve both increased with the temperature. This indicates that temperature had an important influence on the thickness swelling. The higher the temperature, the higher the thickness swelling. K_{SR} and β_{T} of Type E and Type F with the same composition were similar, while those of Type E and Type F were quite different from Type D. This indicates that thickness swelling was closely related to the composition of the composites.

Table 1: Thickness swelling of TBLCs in different hydrothermal environments

Types	Temperature/ $^\circ\text{C}$	Thickness swelling		Fitting for moisture content-strain	
		$K_{\text{SR}}/10^{-2} \text{ s}^{-1}$	R^2	$\beta_{\text{T}} (10^{-2})$	R^2
Type D	25	0.037	0.96	0.19	0.96
	63	1.70	0.95	0.28	0.99
	100	1.80	0.62	0.50	0.94
Type E	25	0.020	0.99	0.29	0.99
	63	0.55	0.99	0.45	0.97
	100	1.43	0.77	0.53	0.99
Type F	25	0.023	0.97	0.29	0.99
	63	0.83	0.99	0.52	0.98
	100	1.01	0.83	0.56	0.95

3.2 Warping of TBLC in Different Hydrothermal Environments

3.2.1 Transverse Warping

The lateral transverse warpage of the three TBLCs under different hydrothermal environments is shown in Fig. 3. The three different structural TBLCs displayed large deformation in the early stage of water absorption. The warpage decreased slightly upon increasing the water absorption time and finally stabilized around an average value. These three TBLCs presented a small fluctuation in their transverse warpage at low temperatures, while a wider range of transverse warpage occurred at high temperatures. In the early stage of water absorption, water entered the composites and mainly existed on the surface of the composites. This caused a moisture content gradient in the thickness direction, which generated internal stress. Combined with the heterogeneity in the thickness direction, this resulted in the warping of the TBLCs. Simultaneously, the composites had residual stress during hot pressing. The entrance of water gradually released internal stress, which also caused warping. As the water continued to move into the internal composites, the moisture content gradient in the thickness direction gradually disappeared, as did the internal stress. This slightly decreased the warpage. Due to the heterogeneity of the TBLC and the

dual effect of humidity and heat, the TBLC was also twisted and deformed. The warpage eventually fluctuated around the average value in the later stage of water absorption.

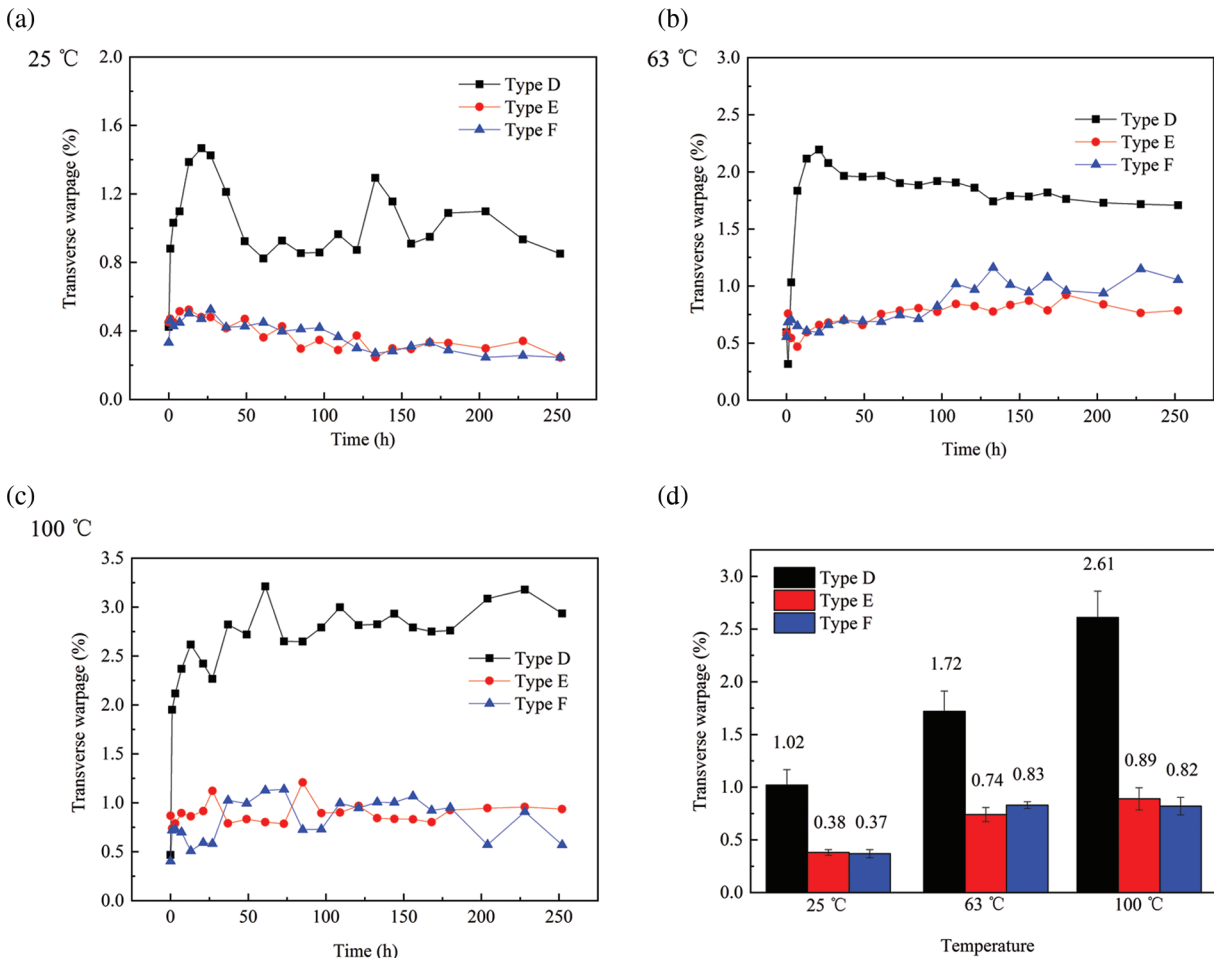


Figure 3: Transverse warpage of TBLCs in 25°C (a), 63°C (b) and 100°C (c) hydrothermal environments. (d) The equilibrium transverse warpage of TBLC under different temperature

Comparing the three different lay-up structural TBLCs shows that the transverse warpage of Type D was much higher than that of Type E and Type F, especially at high temperatures. The transverse warpage of Type D was 2.32 and 2.93 times that of Type E, and 2.07 and 3.18 times that of Type F at 63°C and 100°C, respectively. This illustrates that the transverse wood veneer in the laminate structure hindered the transverse warping deformation of the TBLC. Type E and Type F had a smaller difference in their transverse warpage. As a result, the transverse elements in the lay-up structure reduced the transverse warpage of the TBLC, and Type F had the best resistance to transverse deformation.

3.2.2 Longitudinal Warping

The longitudinal warpage of three structural TBLCs in different hydrothermal environments is shown in Fig. 4. The TBLC displayed large fluctuations in its longitudinal warpage, which was much smaller than the transverse warpage. The longitudinal warpage of Type D and its fluctuation range decreased upon increasing the temperature, while Type E and Type F presented increased longitudinal warpage with the temperature.

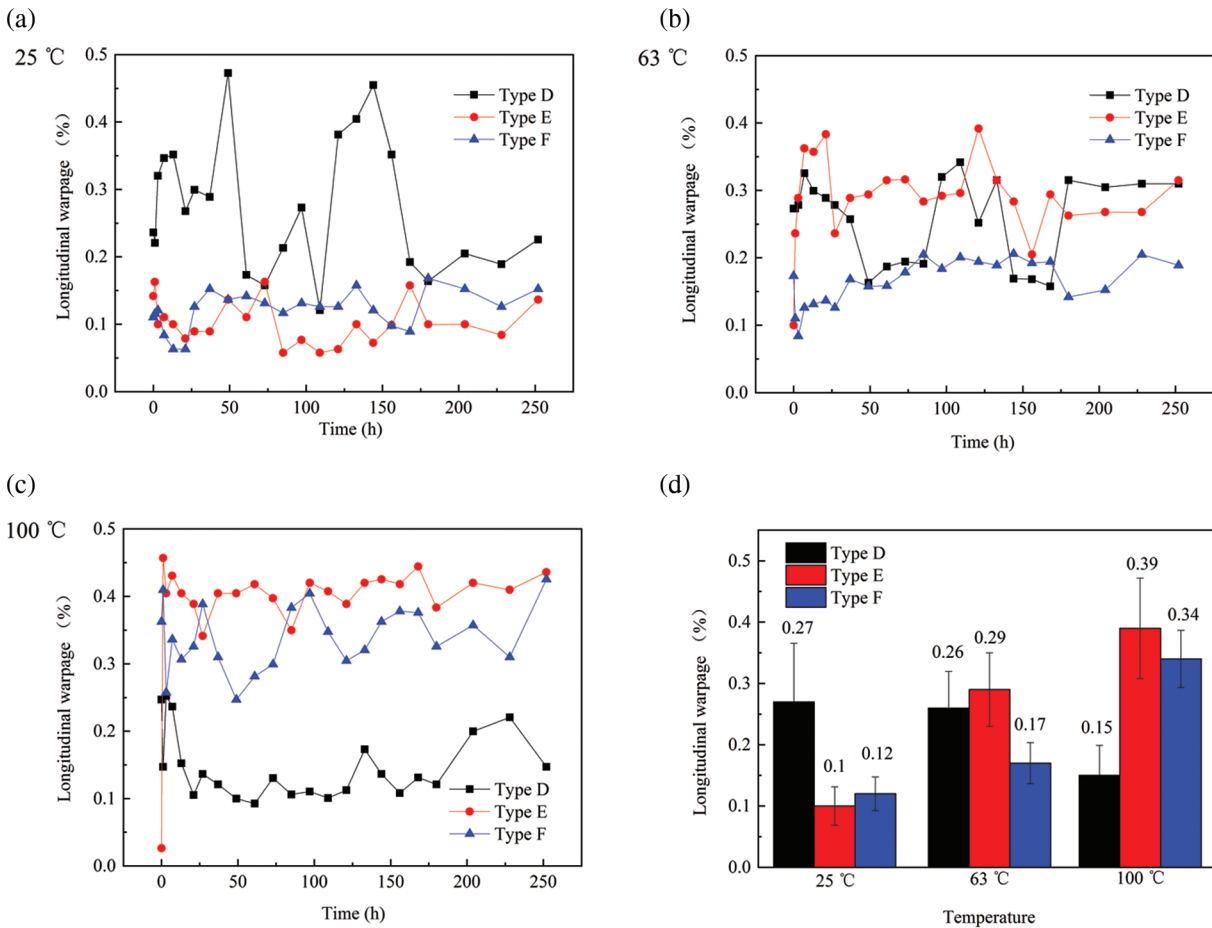


Figure 4: Longitudinal warp deformation of TBLCs in 25°C (a), 63°C (b) and 100°C (c) humidities and temperatures. (d) The equilibrium longitudinal warpage of TBLC under different temperature

Type D had the largest longitudinal warpage at 25°C, which was 2.7 times and 2.25 times higher than that of Type E and Type F, respectively. However, Type E had the largest longitudinal warpage at 63°C and 100°C, which were respectively 1.9 times and 2.9 times higher than that of Type E at 25°C. Type F also presented a gradual increase in longitudinal warpage at 63°C and 100°C, which were 41.67% and 183.33% increases, respectively. However, Type D showed gradually decreased longitudinal warpage at 63°C and 100°C, which were decreases of 37.04% and 44.44%, respectively. This occurred because Type D is a fully-oriented lay-up of bamboo bundle veneer. At the initial stage of water absorption, due to the high moisture content gradient of the TBLC, it underwent large deformation. The moisture content gradient gradually disappeared as water molecules continued moving into the internal composites, which reduced the internal stress. The longitudinal warpage tended to decrease, but Type E and Type F were composed of poplar veneer and bamboo bundle veneer. The transverse and longitudinal hygroscopic swelling coefficients of the wood veneer were larger than those of bamboo in a hydrothermal environment. A higher temperature resulted in a greater difference in the hygroscopic swelling coefficient, which increased the internal stress of the composites. As a result, the longitudinal deformation tended to increase with the temperature. The difference in longitudinal warping between Type E and Type F was mainly caused by their different lay-up structures. Type F had the same number of transverse and longitudinal layers (two layers of wood veneer are regarded as one layer of bamboo veneer), and the symmetrical laminated structure could neutralize the stress caused by the different hygroscopic swelling coefficients. Therefore, Type F had less longitudinal warpage.

3.2.3 Diagonal Warping

Diagonal warpage is an important indicator of the warping of the composites and is affected by the comprehensive influence of the transverse and longitudinal warpage of the composites. The curves of the diagonal warpage of the three different structural types of thin sheets in different hydrothermal environments with water absorption time (Fig. 5) present a consistent trend with the transverse warpage. The warpage rapidly increased at the initial stage of water absorption and then gradually stabilized. The diagonal warpage of the three TBLCs increased with the temperature. Type D had a higher diagonal warpage than Type E and Type F in hydrothermal environments at various temperatures, and the maximum deformation was more than 1.0%. However, Type E and Type F had a small difference in diagonal warpage at 25°C, and the difference between the two became larger as the temperature increased. At 63°C and 100°C, the diagonal warpage of Type E was 1.46 times and 1.54 times higher than that of Type F, respectively. However, the diagonal warpage of the two remained below 1.0%, which meets the requirements of the national standard GB/T 15036-2. For the test results, Type F had better hydrothermal stability and minimal warping.

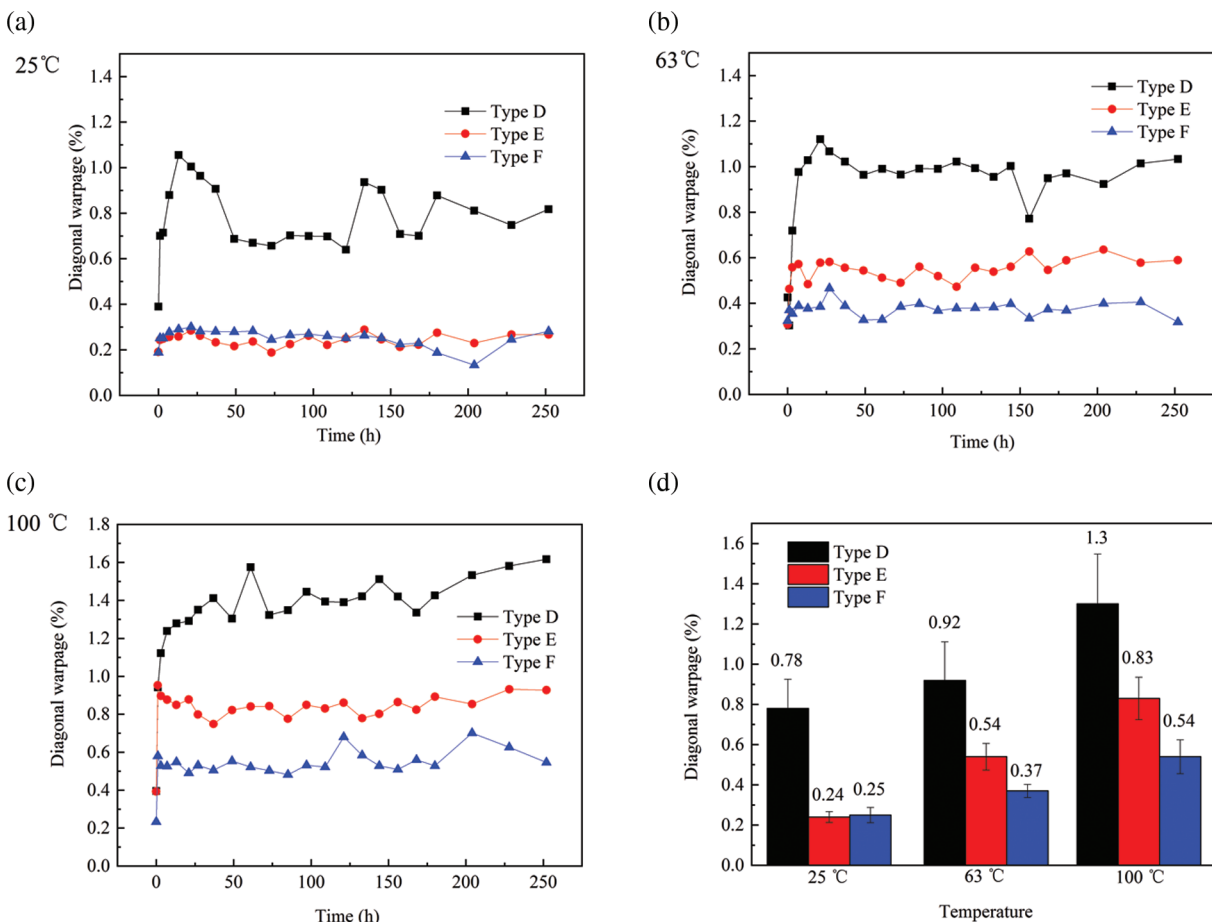


Figure 5: Diagonal warpage of TBLCs in in 25°C (a), 63°C (b) and 100°C (c) hydrothermal environments. (d) The equilibrium diagonal warpage of TBLC under different temperature

3.3 Deformation Mechanism of TBLCs in a Hydrothermal Environment

The deformation of TBLCs in a hydrothermal environment is affected by the comprehensive effects of temperature and water (Fig. 6). In a hydrothermal environment, some microcracks on the surface and inside

the TBLCs are caused by processing. Water enters internal composites through these microcracks [28–30]. Bamboo bundle fibers retained the basic structure of bamboo and were mainly composed of vascular bundles and parenchyma cells. Cellulose and hemicelluloses in bamboo cell wall structure contain hygroscopic groups such as free hydroxyl groups, and water entered the internal composites by passing through these vessels and microcracks. Water was first adsorbed by a large number of hydrophilic groups on the fibers, forming a multi-layer molecular water structure between the molecular chains and increasing the distance between the microfibrils [31–33]. Simultaneously, the temperature acted on the cellulose molecular chains and sugar units, and it made the crystal lattice undergo nonlinear thermal vibration. The higher the temperature, the greater the thermal vibration amplitude of the molecular chains, and the larger the average distance between the molecular chains. This led to linear swelling and volume swelling [34]; however, compared with the influence of temperature and moisture on the deformation of the TBLCs, the thermal expansion caused by temperature was far less than the wet expansion caused by water [22]. Temperature and moisture played a role in the expansion of the TBLC, and the water moved faster in the TBLCs upon increasing the temperature. Under the action of temperature, the phenolic resin adhesive and bamboo bundle fiber showed obvious differences in their thermal expansion and water absorption, which increased interfacial swelling stress and microcracks in the TBLCs [35]. Therefore, this further accelerated the mass transfer process and increased the linear expansion. In a hydrothermal environment, water molecules diffused from the surface layer of the TBLC to the core layer according to Fick's second law in the thickness direction. Due to the high density of the surface layer and the blocking effect of the resin, the surface layer absorbed water and expanded before the subsurface layer and core layer. The surface layer displayed a high swelling per unit thickness. Thus, to maintain the structural stability, the subsurface layer had internal forces that opposed compression of the surface layer and the core layer to the subsurface layer, i.e., the residual stress generated by the humidity gradient. The infiltration of water molecules and thermal expansion damaged the composite interface, which accelerated the release of internal residual stress. This increased the warpage of the TBLC. With the continuous entry of water into the interior of the board, and combined with the temperature, many microcracks and large cracks were generated in the TBLC, which destabilized the structure. The stress-strain relationship in the composite is very complicated and is also the main reason for the fluctuations in the warpage of the composites.

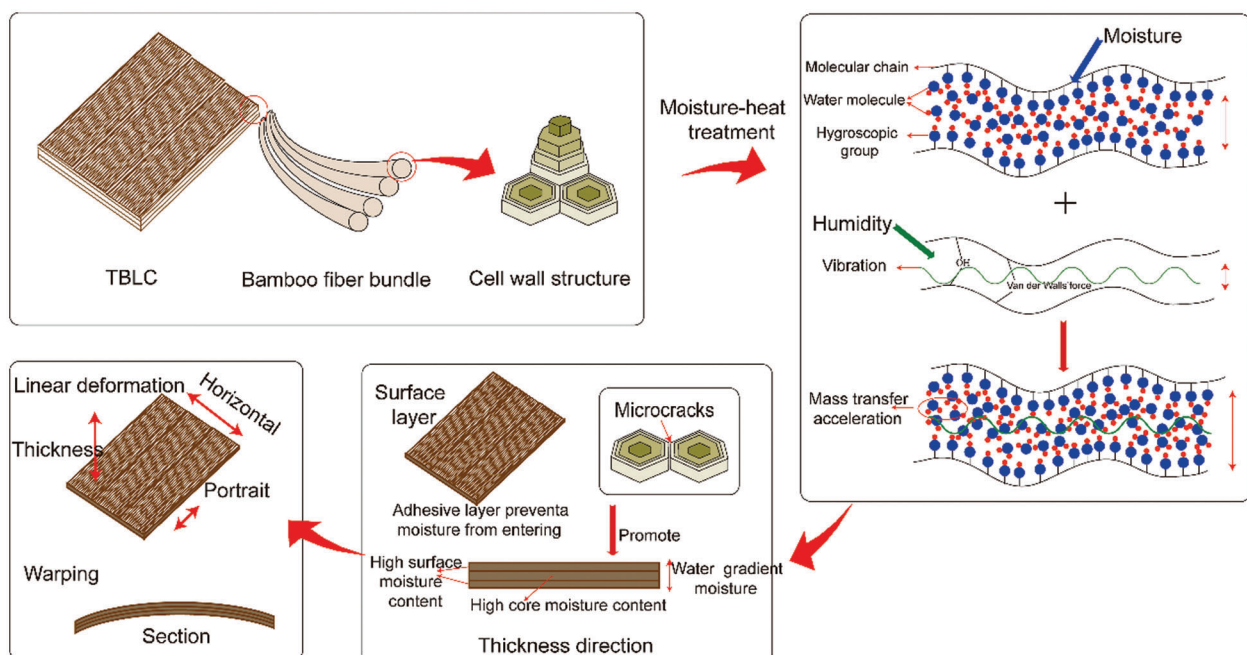


Figure 6: Schematic diagram of the deformation mechanism of TBLC in a hydrothermal environment

4 Conclusions

The linear wet deformation and warpage of thin laminated bamboo bundle veneer composites (TBLCs) with different lay-up structures in different hydrothermal environments were investigated in this study. A thickness swelling model was used to model the thickness swelling of the TBLC and was used to explain the linear wet deformation mechanism of the TBLC.

The linear deformation of the TBLC increased with the temperature, and Type E presented a 3.22 times increase in thickness swelling at 100°C compared with at 25°C. Type E and Type F displayed greater thickness swelling than Type D. The fitting curve of the thickness swelling exhibited a better fit at a lower temperature and a larger deviation at high temperatures. Internal stress developed in the TBLC due to heterogeneity in the thickness direction and the existence of a moisture content gradient in the thickness direction. This was the main reason for the warping. TBLC displayed less longitudinal warpage than transverse warpage. Type D presented a much higher transverse warpage than Type E and Type F, while the difference in transverse warpage of Type E and Type F was smaller.

The transverse elements in the lay-up structure reduced the transverse warpage. Type D had the largest longitudinal warpage at low temperatures, and Type F had less longitudinal warpage. Type D had greater diagonal warpage than Type E and Type F in a hydrothermal environment at different temperatures, and their maximum deformation was more than 1.0%. However, Type E and Type F had a diagonal warpage below 1.0%, which meets the requirements of the GB/T 15036-2. Type F had a twist of 0.12% at 25°C, which was 80% and 66.7% times lower than that of Type D and Type E, respectively.

Acknowledgement: The technical guidance from International Centre for Bamboo and Rattan is gratefully acknowledged. The authors would also like to thank Fujian Youzhu Technology Co., Ltd. for supplying the raw materials.

Funding Statement: This research was financially supported by the Youth Top-notch Talent Program of Science and Technology Innovation for Forestry and Grassland (2019132606).

Conflicts of Interest: The authors declare that they have no conflicts of interest to report regarding the present study.

References

1. Wang, G., Chen, F. (2017). Development of bamboo fiber-based composites. *Advanced High Strength Natural Fibre Composites in Construction*, 235–255. DOI 10.1016/B978-0-08-100411-1.00010-8.
2. Huang, Y., Qi, Y., Zhang, Y., Yu, W. (2019). Progress of bamboo recombination technology in China. *Advances in Polymer Technology*, 2019. DOI 10.1155/2019/2723191.
3. Yang, W., Zhao, K., Chen, H., Chen, S., Ding, M. (2020). Experimental study on the creep behavior of recombinant bamboo. *Journal of Renewable Materials*, 8(3), 251–273. DOI 10.32604/jrm.2020.08779.
4. Shu, B., Xiao, Z., Hong, L., Zhang, S., Li, C. et al. (2020). Review on the application of bamboo-based materials in construction engineering. *Journal of Renewable Materials*, 8(10), 1215–1242. DOI 10.32604/jrm.2020.011263.
5. Zhang, Y., Yu, W., Kim, N., Qi, Y. (2021). Mechanical performance and dimensional stability of bamboo fiber-based composite. *Polymers*, 13(11), 1732. DOI 10.3390/polym13111732.
6. Rao, F., Ji, Y., Li, N., Zhang, Y., Chen, Y. et al. (2020). Outdoor bamboo-fiber-reinforced composite: Influence of resin content on water resistance and mechanical properties. *Construction and Building Materials*, 261, 120022. DOI 10.1016/j.conbuildmat.2020.120022.
7. Zhou, J., Li, C. Y., Zhang, Y., Dai, J. (2009). Three 1-D selenidogallates $[\text{GaSe}_2^-]_n$, displaying conformational variations. *Journal of Coordination Chemistry*, 62(7), 1112–1120. DOI 10.1080/00958970802468617.

8. Tamrakar, S., Lopez-Anido, R. A. (2011). Water absorption of wood polypropylene composite sheet piles and its influence on mechanical properties. *Construction and Building Materials*, 25(10), 3977–3988. DOI 10.1016/j.conbuildmat.2011.04.031.
9. Pendleton, D. E., Hoffard, T. A., Adcock, T., Woodward, B., Wolcott, M. P. (2002). Durability of an extruded HDPE/wood composite. *Forest Products Journal*, 52(6), 21–27.
10. Shi, S. Q., Gardner, D. J. (2006). Hygroscopic thickness swelling rate of compression molded wood fiberboard and wood fiber/polymer composites. *Composites Part A: Applied Science and Manufacturing*, 37(9), 1276–1285. DOI 10.1016/j.compositesa.2005.08.015.
11. Shi, S. Q. (2007). Diffusion model based on fick's second law for the moisture absorption process in wood fiber-based composites: Is it suitable or not? *Wood Science and Technology*, 41(8), 645–658. DOI 10.1007/s00226-006-0123-4.
12. Kazemi Najafi, S., Kiaefar, A., Tajvidi, M. (2008). Effect of bark flour content on the hygroscopic characteristics of wood–polypropylene composites. *Journal of Applied Polymer Science*, 110(5), 3116–3120. DOI 10.1002/app.28852.
13. Kazemi Najafi, S., Mostafazadeh-Marznaki, M., Chaharmahali, M. (2010). Effect of thermo-mechanical degradation of polypropylene on hygroscopic characteristics of wood flour-polypropylene composites. *Journal of Polymers and the Environment*, 18(4), 720–726. DOI 10.1007/s10924-010-0220-1.
14. de Freitas, V. P., Delgado, J. M., Machado, N. (2015). Wood dimensional changes due to hygrothermal behaviour. *Defect and Diffusion Forum*, 365, 172–177. DOI 10.4028/www.scientific.net/DDF.365.172.
15. Gigliotti, M., Minervino, M., Grandidier, J. C., Lafarie-Frenot, M. C. (2012). Predicting loss of bifurcation behaviour of 0/90 unsymmetric composite plates subjected to environmental loads. *Composite Structures*, 94(9), 2793–2808. DOI 10.1016/j.compstruct.2012.03.017.
16. Betts, D. N., Kim, H. A., Bowen, C. R. (2012). Optimization of stiffness characteristics for the design of bistable composite laminates. *AIAA Journal*, 50(10), 2211–2218. DOI 10.2514/1.J051535.
17. Cui, H. X., Guan, M. J., Zhu, Y. X., Zhang, Z. Z. (2012). The flexural characteristics of prestressed bamboo slivers reinforced parallel strand lumber (PSL). *Key Engineering Materials*, 517, 96–100. DOI 10.4028/www.scientific.net/KEM.517.96.
18. Duan, Y., Zhang, J., Tong, K., Wu, P., Li, Y. (2021). The effect of interfacial slip on the flexural behavior of steel-bamboo composite beams. *Structures*, 32, 2060–2072. DOI 10.1016/j.istruc.2021.04.019.
19. Shirmohammadi, M., Leggate, W., Redman, A. (2021). Effects of moisture ingress and egress on the performance and service life of mass timber products in buildings: A review. *Construction and Building Materials*, 290, 123176. DOI 10.1016/j.conbuildmat.2021.123176.
20. Yuan, J., Fang, C., Chen, Q., Fei, B. (2021). Observing bamboo dimensional change caused by humidity. *Construction and Building Materials*, 309, 124988. DOI 10.1016/j.conbuildmat.2021.124988.
21. Telford, R., Katnam, K. B., Young, T. M. (2014). The effect of moisture ingress on through-thickness residual stresses in unsymmetric composite laminates: A combined experimental–numerical analysis. *Composite Structures*, 107, 502–511. DOI 10.1016/j.compstruct.2013.08.008.
22. Guan, M. J., Zhang, Q. S. (2016). Hygrothermal effects of bamboo by dynamic mechanical analysis. *Journal of Nanjing Forestry University*, 49(1), 65.
23. Gereke, T., Hass, P., Niemz, P. (2010). Moisture-induced stresses and distortions in spruce cross-laminates and composite laminates. *Holzforschung*, 64(1), 127–133. DOI 10.1515/HF.2010.003.
24. Zhou, H., Wei, X., Smith, L. M., Wang, G., Chen, F. (2019). Evaluation of uniformity of bamboo bundle veneer and bamboo bundle laminated veneer lumber (BLVL). *Forests*, 10(10), 921. DOI 10.3390/F10100921.
25. Yu, Y., Huang, Y., Zhang, Y., Liu, R., Meng, F. et al. (2019). The reinforcing mechanism of mechanical properties of bamboo fiber bundle-reinforced composites. *Polymer Composites*, 40(4), 1463–1472. DOI 10.1002/pc.24885.
26. Jain, D., Zhao, Y. Q., Batra, R. C. (2020). Analysis of three-dimensional bending deformations and failure of wet and dry laminates. *Composite Structures*, 252, 112687. DOI 10.1016/j.compstruct.2020.112687.
27. Chen, Q., Fang, C., Wang, G., Ma, X., Chen, M. et al. (2020). Hygroscopic swelling of moso bamboo cells. *Cellulose*, 27(2), 611–620. DOI 10.1007/s10570-019-02833-y.

28. Zhou, H., Wang, G., Chen, L., Yu, Z., Smith, L. M. et al. (2019). Hydrothermal aging properties of three typical bamboo engineering composites. *Materials*, 12(9), 1450. DOI 10.3390/ma12091450.
29. Lou, Z., Han, X., Liu, J., Ma, Q., Yan, H. et al. (2021). Nano-Fe₃O₄/bamboo bundles/phenolic resin oriented recombination ternary composite with enhanced multiple functions. *Composites Part B: Engineering*, 226, 109335. DOI 10.1016/j.compositesb.2021.109335.
30. Chen, M., Ye, L., Semple, K., Ma, J., Zhang, J. et al. (2022). A new protocol for rapid assessment of bond durability of bio-based pipes: Bamboo winding composite pipe as a case study. *European Journal of Wood and Wood Products*, 80, 947–959. DOI 10.1007/s00107-022-01808-4.
31. Shen, Y., Zhong, J., Cai, S., Ma, H., Qu, Z. et al. (2019). Effect of temperature and water absorption on low-velocity impact damage of composites with multi-layer structured flax fiber. *Materials*, 12(3), 453. DOI 10.3390/ma12030453.
32. Jin, Q., Zhu, L., Hu, D., He, C., Li, L. (2021). Nuclear magnetic resonance analysis of water absorption characteristics and dynamic changes in pore size distribution of wood-plastic composites. *BioResources*, 16(2). DOI 10.15376/BIORES.16.2.4064-4080.
33. Zhang, C. (2020). *Hygromechanics and shape memory of wood cell wall investigated with multiscale modeling (Ph.D. Thesis)*. ETH Zurich. DOI 10.3929/ethz-b-000452831.
34. Prabhudass, J. M., Palanikumar, K., Natarajan, E., Markandan, K. (2022). Enhanced thermal stability, mechanical properties and structural integrity of MWCNT filled bamboo/Kenaf hybrid polymer nanocomposites. *Materials*, 15(2), 506. DOI 10.3390/ma15020506.
35. Uyup, M. K. A. (2008). *Impregnation of bamboo (Gigantochloa scortechinii) with phenolic resin for the production of dimensionally stable plybamboo (Ph.D. Thesis)*. Universiti Putra Malaysia.